Oxidation of Elemental Mercury by Chlorine: Gas Phase, Surface, and Photo-induced Reaction Pathways

NAI-QIANG YAN[+], SHOU-HENG LIU[≠] AND SHIH-GER CHANG[*]
Environmental Energy Technology Division, Lawrence Berkeley National Laboratory, University of California, Berkeley, California 94720.

Abstract

Accurate oxidation rate constants of mercury gas are needed for determining its dispersion and lifetime in the atmosphere. They would also help in developing a technology for the control of mercury emissions from coal-fired power plants. However, it is difficult to establish the accurate rate constants primarily due to the fact that mercury easily adsorbs on solid surface and its reactions can be catalyzed by the surface. We have demonstrated a procedure that allows the determination of gas phase, surface-induced, and photo-induced contributions in the kinetic study of the oxidation of mercury by chlorine gas. The kinetics was studied using reactors with various surface to volume ratios. The effect of the surface and the photo irradiation on the reaction was taken into consideration. The pressure dependent study revealed that the gas phase oxidation was a three-body collision process. The third order rate constant was determined to be $7.5(\pm 0.2)\times 10^{-39}$ $mL^2 \cdot molecules^{-2} \cdot s^{-1}$ with N_2 as the third body at $297\pm 1^{\circ}K$. The surface induced reaction on quartz window was second order and the rate constant was 2.7×10^{-17} $mL^2 \cdot molecules^{-1} \cdot cm^{-2}$ sec. Meanwhile, the 253.7 nm photon employed for mercury detection was found to accelerate the reaction. The utilization efficiency of 253.7 nm photon for Hg^0 oxidation was 6.7×10^{-4} $molecules \cdot photon^{-1}$ under the conditions employed in this study.

+ On leave from the School of Environmental Science and Engineering, Shanghai Jiao Tong University, PRC
≠ On leave from Environmental Engineering Department, Taiwan Cheng-Kung University, Tainan, Taiwan, ROC
* Corresponding author phone: (510) 486-5125; Fax: (510) 486-7303; e-mail:sgchang@lbl.gov.

Introduction

Mercury is a leading concern among the air toxic metals (1, 2). Once it is introduced into an ecosystem, it will stay in the food chain (3). In the aquatic environment mercury can be converted by microbial action to methylmercury (4), which is more toxic to humans, especially to children and developing fetuses, causing irreversible neurological damage. Mercury also has been linked to autoimmune disorders, hypertension, and cardiovascular disease. Mercury poisonings from the exposures to methylmercury in fish have been documented (2,5).

Among human activities, coal fired power plants represent the primary mercury emission source. Although the levels of mercury in coal are small (0.04-0.53 $mg \cdot kg^{-1}$) (6-9), the amount of coal burn is huge. It is known that all the mercury in coal is converted to the elemental form (Hg^0) in the high-temperature combustion zone and that oxidation may occur as the combustion gases cool and Hg^0 interacts with constituent gases and particulate matter in the gas stream. Hg^0 is most difficult to capture because it is volatile and insoluble in water. If it is released to the atmosphere, it can remain aloft for months, spreading over vast regions of the globe (10). Unlike Hg^0, the oxidized mercury, in the form of mercuric or mercurous salts, is much less volatile and more soluble in water (11). As a result, it can be readily washed out by rain, resulting in a short lifetime in the atmosphere (12-15). Also, it can be more easily captured by existing coal utility pollution control equipments, such as baghouse/ESP (electrostatic precipitator) or wet SO_2 scrubbers (16-18). However, the kinetics of the oxidation of Hg^0 in the atmosphere and in the power plant flue gas system is still not well understood (12,14,15). Although a few gas phase reactions involving Hg^0 have been studied, many of them reported only the upper limit of rate constants (19-21). This is because the gas phase oxidation of Hg^0 is

difficult to study due to the fact that the Hg^0 easily adsorbs on solid surface and its reactions can be catalyzed by the surface (11,14,15). Consequently, any analytical instrument for Hg^0 determination could produce erroneous results if it requires the transfer of samples (15). Also, the 253.7 nm photons, which are used to monitor the Hg^0 concentration, can accelerate the reactions as will be demonstrated in this study.

In this paper, we design experiments to separate, for the first time in the kinetic study of Hg^0 reactions, the contribution of each of three concurrent mechanisms in the oxidation of Hg^0 by chlorine (Cl_2). The three concurrent mechanisms include the gas phase, surface and photo-induced oxidation of Hg^0 by Cl_2. The motivation of studying the oxidation of Hg^0 by Cl_2 is because chlorine exists in coal (1,6,7) as well as in the atmosphere (15).

Experimental Section

Apparatus.

The apparatus (Figure 1) used for kinetic studies includes a self-assembled cold vapor atomic absorption spectrophotometer (CVAAS), glass reactor (Pyrex), and vacuum system for gas handling. A low-pressure mercury lamp (Oriel, Model 6035) was used as the 253.7 nm uv light source. The light beam was collimated with lens before passing the reactor through the quartz windows. The light after passing the reactor was detected by a photodiode (Edmund, Model NT54-037). The intensity data as a function of time were recorded in a computer via an A/D converter (DataQ, Model DI-700).

The Pyrex reactors used for the kinetic study were spherical and oval shapes with two short necks (dia. 20.5 mm, length 18 mm) connected for attaching quartz windows. Three sizes of reactors with different surface to volume ratios were employed for determining the contribution of the surface and photo-induced reactions. The volume of the three reactors was 190, 380, and 960 mL, with a surface area of 190, 255, and 498 cm^2, respectively, corresponding to the ratio of the volume to the surface area of 1, 1.49, and 1.93 $mL \cdot cm^{-2}$. The surface area of quartz windows and optical path, which were identical for all the three reactors, were 6.6 cm^2 and 14.5 cm, respectively. The reactors could be readily exchanged from one another in the assembly. The reactor was cleaned with nonionic water frequently to minimize the effect of the product on the wall. All the inner wall of Teflon gas tubes and valves connected to the reactors were coated with halocarbon wax (HW) to minimize the Hg^0 adsorption.

Chemicals. The chlorine (calibrated standard gas of 5000 ppm with N_2 the balance) and nitrogen (high purity grade) were from Airgas Co.. Halocarbon wax (HW, Series-1500) was from Halocarbon Product Co.. Mercury (99.99%), H_2SO_4 (98%), $K_2C_2O_4$ (99%), $FeCl_3 \cdot 6H_2O$ (98%), $FeSO_4 \cdot 7H_2O$ (99%) and 1,10-phenanthroline (95%) were from Sigma-Aldrich.

Procedures. The kinetics was performed using the absolute rate technique under pseudo-first-order condition with respect to Hg^0. The Hg^0 and Cl_2 were introduced into the reactor by injection with a syringe. Initially, the reactor was evacuated and then a volume of nitrogen gas saturated with Hg^0 was injected with a syringe (B-D Yale, 100 mL) to the reactor to reach a pressure of about 250 Torr (1 atm.=760 Torr). The pressure in the reactor was then brought up to 500 Torr with nitrogen gas. Subsequently, a volume of known concentration of Cl_2 in nitrogen

was injected by a syringe into the reactor before the pressure was quickly brought to 760 Torr with nitrogen. The concentration of Cl_2 was measured at 330 nm with a uv-visible spectrophotometer (Perkin Elmer, Lambda-02). Nitrogen instead of air was used as the balance gas to avoid the mercury photosensitized reaction because of oxygen (17,22). The reactor was cleaned with nonionic water after each run to minimize the possible effect of the products deposited on the wall from the previous run.

The rate of disappearance of Hg^0 in the reactors was monitored at 253.7 nm by CVAAS during the course of the reaction. However, the loss of Hg^0 in the reactor as measured by the CVAAS could come from several reaction pathways: 1. adsorption on reactor wall and quartz window, 2. gas phase reaction, 3. surface-induced reaction, and 4. photo-induced reaction.

The adsorption of Hg^0 on the wall was investigated by performing an experiment without chlorine while monitoring the concentration decay of the Hg^0 in the reactor as a function of time. The effect of 253.7 nm photons on the reaction rate was studied by comparing the Hg^0 decay rate between a continuous irradiation and intermittent irradiation. In the intermittent irradiation, the 253.7 nm light was blocked from entering the reactor most of the time until a reading of Hg^0 concentration was taken, which occurred periodically and each time lasted only a few seconds.

The adsorption of Hg^0 on the wall can be minimized by coating the wall with HW. However, the quartz windows cannot be coated with HW because it attenuates 253.7 nm light. To determine the Hg^0 loss from the adsorption on the windows and the gas phase reaction, experiments were performed with three reactors having different ratio of window surface area to the reactor

volume. Since the experiments were performed in the intermittent irradiation mode, the gas phase reaction rate constant without the influence of 253.7 nm photon can be obtained.

The loss of Hg^0 due to the reaction of photo-excited Hg^0 with Cl_2 was examined. Two sets of experiments were conducted: one with a continuous irradiation and the other with an intermittent irradiation. The difference between the results of these two sets of experiments allows the determination of the contribution due to the photo-induced gas phase and photo-induced surface reaction on windows.

The light intensity was measured by a thermopile (Eppley, Serial no. 16034E6) and chemical actinometry method employing Potassium Ferrioxalate (22). The average intensity measured at the reactor was 6.06×10^{16} photons$\cdot cm^{-2}\cdot s^{-1}$, and was in good agreement between both methods.

Result and Discussion

Adsorption on the wall. The adsorption of Hg^0 on the wall was investigated, without Cl_2 in three reactors at 297±1°K. Figure 2 shows that the rate of the adsorption of Hg^0 on the wall (Pyrex) without coating was very significant. The Hg^0 initial concentration, $[Hg^0]_0$, was 0.18 ppm (1ppm = 2.46×10^{13} molecules$\cdot mL^{-1}$ at 297°K). About 41% and 20% of Hg^0 originally in the gas phase had adsorbed on the wall of the small and large reactor, respectively, after 300 sec. The adsorption rate decreased substantially if the wall had been coated with HW. Only 11%, 7% and 4% of Hg^0 had adsorbed on the wall in the small, medium and large reactors after 300 sec, respectively.

Additionally, it was observed that the adsorption rate of Hg^0 displayed an exponential decay curve, which can be described by the 1st order kinetic equation.

$$\Sigma A_a R_a = (A_q k_{aq} + A_w k_{aw})[Hg^0] \qquad (1)$$

where R_a (molecules·cm^{-2}·s^{-1}) is the Hg^0 adsorption rate, k_{aq} and k_{aw} (mL·cm^{-2}·s^{-1}) represent the adsorption rate constant on quartz and halocarbon wax coated wall surfaces, respectively. A_q and A_w are the area of quartz windows and the HW coated reactor wall, respectively. $A_w k_{aw}$ should be replaced by $A_p k_{ap}$ if the Pyrex wall was not coated with HW. By measuring the rate of the disappearance of Hg^0 in three reactors, the adsorption rate constants were calculated to be 1.4×10^{-3}, 1.7×10^{-3} and 2.5×10^{-4} mL·cm^{-2}·s^{-1} for the quartz, Pyrex and HW coated wall surfaces, respectively. The Hg^0 adsorption rate constant on the HW coated wall is almost an order of magnitude smaller than that on the wall without the coating.

Whether the adsorbed Hg^0 on the quartz window will attenuate the light intensity (253.7 nm photons) and interfere with the kinetic study of Hg^0 with Cl_2 was assessed. The Hg^0 concentration employed was 4.4×10^{12} molecules·mL^{-1} (0.18 ppm). The total number of Hg^0 initially introduced into the small (190 mL), medium (380 mL), and large (960 mL) reactors was 9.2×10^{14}, 1.84×10^{15}, and 4.65×10^{15} molecules, respectively. From the adsorption rate constant on the quartz window, the number of Hg^0 adsorbed on the quartz window was calculated to be 7.05×10^{12} molecules after 300 sec, which was the time period when most of the kinetic data were collected. Therefore, less than one hundredth of the Hg^0 initially introduced adsorbed on the quartz window during the course of the reaction. Also, the number of Hg^0 required to cover one monolayer on the quartz window (6.6 cm^2) was estimated to be 9.34×10^{15} molecules. Therefore, the Hg^0 adsorbed on the window in 300 sec was less than one thousandth of a monolayer. Using

the absorption cross section of Hg^0, $\sigma = 4.5\times10^{-16}$ $cm^2\cdot molecules^{-1}$ at 253.7 nm (23), and assuming one thousandth of a monolayer of Hg^0 adsorbed on the quartz surface, the light attenuated by the adsorbed Hg^0 is only 0.05%, which is negligible in this kinetic study.

The effect of pressure on the Hg^0 adsorption rate was studied. We found that the adsorption rate is proportional to the total gas pressure in the reactor. With the same initial Hg^0 concentration of 4.4×10^{12} molecules$\cdot mL^{-1}$, but by reducing the gas pressure from 1 atm. to 245 Torr, the loss of Hg^0 in gas phase decreased to about 4% and 1% in the small and large reactors, respectively, after 300 sec.

The overall Hg^0 depletion rate. The typical depletion curves of Hg^0 in the presence of Cl_2 under various experimental conditions were depicted in Figure 3. The initial concentration of Hg^0 and Cl_2 in all the runs was 4.4×10^{12} and 6.5×10^{15} molecules$\cdot mL^{-1}$, respectively, with the balance N_2 gas to 1 atm. Experiments were performed at 297 ± 1^oK. The Hg^0 depletion rate was rather rapid when the reactor wall was not coated with the HW (compare curve 1 and 2, given the same small reactor), which suggests that in addition to the much slower adsorption rate (Figure 2), the Pyrex wall catalyzed the reaction of Hg^0 with Cl_2. The present of the photo-induced reaction is obvious from the fact that the Hg^0 depletion rate is faster in runs under the continuous (curve 4) than the intermittent (curve 5) irradiation.

Even under the conditions where the Pyrex reactor wall was coated with HW and that the reactions proceeded in the dark, the depletion rate of Hg^0 was faster in the small reactor (curve 3) than that in the larger one (curve 5). This result indicates that the surface of quartz window and the reactor wall after coating the HW should still contribute to the depletion of Hg^0. The

magnitude of the Hg^0 depletion from reactions on the quartz window, the HW coated reactor wall, and in the gas phase can be calculated by conducting experiments in three reactors with different surface to volume ratios as discussed before.

The depletion of Hg^0 under all experimental conditions follows a 1st order reaction rate law with respect to Hg^0, as can be seen when plotting logarithm of the relative Hg^0 concentration over the reaction time (Figure 3). Thus, the over-all depletion rate of Hg^0 can be expressed by eq 2.

$$-d[Hg^0]/dt = k_T[Hg^0] \qquad (2)$$

where k_T is the apparent overall depletion rate constant, s^{-1}. $[Hg^0]$ is the concentration of Hg^0 in the gas phase, molecules·mL^{-1}.

The fact that the overall Hg^0 depletion rate follows a 1st order rate equation can be used to suggest that individual Hg^0 depletion pathways involved also follow a 1st order rate equation. The logic of this suggestion is underway. When the experiment was conducted in a reactor with HW coating and in the dark (e.g. curve 3 and 5), the overall Hg^0 depletion in the reactor constitute three pathways: the gas phase reaction, adsorption and reaction on the surface. The gas phase reaction of Hg^0 with Cl_2 can be regarded as the pseudo-first order reaction with respect to Hg^0 because the concentration of Cl_2 was much larger than that of Hg^0. The adsorption rate was proportional to the Hg^0 concentration as demonstrated (eq 1). Consequently, the remaining surface reaction pathway must follow the first-order rate law, given the fact that its contribution to the total Hg^0 depletion is very significant. Likewise, the photo-induced reaction and the reaction on the Pyrex surface can be considered as the first-order reaction from the curve 1, 2, and 4 in Figure 3.

Based on the aforementioned analysis, the overall rate of the disappearance of Hg^0 (eq 2) can be further expressed with eq 2a, in which the surface adsorption is combined with the surface reaction as it will be treated as one pathway in depleting the Hg^0 from the gas phase.

$$-d[Hg^0]/dt=[k_g^{'}+ k_p^{'}(V_p/V) +\alpha_q(k_{aq}+k_{sq}^{'}) A_q/V + \alpha_w(k_{aw}+k_{sw}^{'}) A_w/V] [Hg^0] \quad (2a)$$

where V_p is the volume of gas in the reaction that was illuminated by the light, and V is the total volume of the reactor. $k_g^{'}$, $k_p^{'}$ represent the pseudo-first-order rate constants of gas phase and photo-induced reaction, s^{-1}; $k_{sq}^{'}$ and $k_{sw}^{'}$ are the pseudo-first-order rate constants of surface reaction on the quartz and halocarbon wax coated surface, $mL\cdot s^{-1}\cdot cm^{-2}$.

α_q or α_w equals to $[Hg^0]_s/[Hg^0]$, which is a concentration distribution coefficient (≤ 1) between the local gas concentration on the surface, $[Hg^0]_s$, and the bulk gas concentration of Hg^0, and it will be discussed further later (see eq 8). *A* with different subscripts represents the corresponding surface area in the reactor.

Based on eq 1 and 2a, the overall rate constant, k_T, can be expressed as follows.

$$k_T = k_g^{'}+ (V_p/V) k_p^{'} +\alpha_q(k_{aq}+k_{sq}^{'}) A_q/V + \alpha_w (k_{aw}+k_{sw}^{'}) A_w/V \quad (3)$$

k_T was obtained directly from the experiment. However, series of experiments must be performed to determine the contributions of each reaction pathways and to evaluate the corresponding rate constants.

Gas phase reaction rate. To minimize the photo-induced reaction, the light was allowed to pass through the reactor for Hg^0 measurement about 2 secs for every 40-60 secs of reaction. Thus the effect of uv was trifling and the second term in the eq 3 can be neglected ($V_p=0$). The wall of the reactor was coated with HW except the quartz windows. Thus, eq 3 can be reduced to

$$k_T =k_g^{'}+\alpha_q(k_{aq}+k_{sq}^{'}) A_q/V + \alpha_w(k_{aw}+k_{sw}^{'}) A_w/V \quad (4)$$

where the subscript s*q* and s*w* represent the surface of quartz windows and HW coated reactor wall, respectively. The three terms in the right of eq 4 represent the contribution of gas phase reaction, quartz surface and HW coated reactor wall, respectively.

The terms, k_g', $\alpha_q(k_{aq}+k_{sq}')$, and $\alpha_w(k_{aw}+k_{sw}')$ in eq 4 can be calculated from k_T by performing reactions in three reactors with different surface to volume ratios, the results are shown in Table 1.

The calculated value of $\alpha_q(k_{aq}+k_{sq}')$ for quartz surface was much larger than the adsorption rate constant k_{aq} (about 1.4×10^{-3} mL·cm^{-2}·s^{-1} as indicated before), implying that the surface reaction rate was more rapid than the adsorption rate. Consequently, the adsorption on quartz surface was neglected, and $\alpha_q k_{sq}'$ was used in Table 1 instead of $\alpha_q(k_{aq}+k_{sq}')$.

On the contrary, the value of $\alpha_w(k_{aw}+k_{sw}')$ for HW coated surface (Table 1) was about the same as the adsorption rate constant k_{aw} (0.25×10^{-3} mL·cm^{-2}·s^{-1}), suggesting that the surface reaction on the HW coated surface was slow. Therefore, the contribution of surface reaction on the HW coated reactor wall was neglected.

Meanwhile, the results (Table 1) show that the contribution of gas phase reaction to the overall reaction, k_g'/k_T, was smaller in the small reactor than the larger one as it should be expected. For example, the percentage of the pseudo first order gas phase rate constant to the over-all rate constant, k_g'/k_T was determined to be 21.0%, 34.4%, and 58.7% for reactors with 190 mL, 380 mL, and 960 mL volume, respectively, at a Cl_2 concentration of 2.5×10^{15} molecules·mL^{-1} (Table 1).

Also, the relative contribution of the gas phase reaction increases with an increase of Cl_2 concentration (Table 1), given the same reactor. For example in the 960 mL reactor, k_g'/k_T was 50.5%, 58.7%, and 71.1% with [Cl_2] of 1.3×10^{15}, 2.5×10^{15} and 6.5×10^{15} molecules·mL^{-1},

respectively. This is because the surface reaction rate is determined by both the chemical reaction rate and the rate of Hg^0 diffusion from the bulk to the surface. A detail discussion and mathematical equation (eq10) will be presented later.

Additionally, k_g' were proportional to the concentration of Cl_2 (Table 1), which indicates that the gas phase reaction rate is over-all a 2nd order, having 1st order with respect to both Hg^0 and Cl_2. The gas phase reaction rate constants of Hg^0 with Cl_2 determined from various conditions in three reactors were in very good agreement and averaged at 1.82×10^{-19} mL·molecules^{-1}·s^{-1} at 1 atm and 297±1 ^oK.

The effect of gas pressure on the reaction rate was studied. Figure 4 shows the overall pseudo-1st order rate constant, k_T as a function of pressure. The Hg^0 and Cl_2 concentrations in all the runs were 4.4×10^{12} and 6.5×10^{15} molecules·mL^{-1}, respectively. The balance of the gas in the reactor was nitrogen. It can be seen that the k_T increased with the decrease of the pressure in the small reactor. On the contrary, k_T decreased with the decrease of the gas pressure in the large reactor. This behavior can be explained as follow: The small reactor has a larger surface component because it has a larger surface to volume ratio compared to the larger reactor. The surface reaction on the quartz is more favorable at a reduced pressure due to the increase of the diffusion coefficient, which is inversely proportional to the gas pressure (24,25). However, the gas phase reaction rate would decrease with the decrease of the pressure if it goes through a third body collision process. Another words, there are two reaction mechanisms taking place simultaneously; one would show an increase with a decrease of the total pressure, but the other would show a decrease with a decrease of the pressure. Figure 4 shows the effect of the pressure on the pseudo-1st order over-all rate constant, i.e. the sum of the two reaction mechanisms, in

three reactors. Therefore, the overall rate constant should increase with the decrease of the pressure if the surface reaction is dominant, such as the case in a small reactor.

Similarly, by performing experiments in three reactors under different gas pressure, k_g' and $\alpha_q k_{sq}'$ were calculated (Table 2) from the k_T values obtained experimentally. It was obvious that the apparent surface reaction rate constant, $\alpha_q k_{sq}'$, on the quartz increased with the decrease of the gas pressure. Whereas, the pseudo-1st order gas phase rate constant k_g' showed a linear dependence on the gas pressure. This implies that the gas phase reaction of Hg^0 and Cl_2 can be regarded as a three-body collision reaction.

$$Hg^0 + Cl_2 + M \rightarrow HgCl_2 + M \qquad (5)$$

$$R_g = k_g'[Hg^0] = k_g[Cl_2][Hg^0] = k_3[M][Cl_2][Hg^0] \qquad (6)$$

where M represents the third body, which is N_2 in this case. The third-order gas phase reaction rate constant, k_3, was determined to be $7.5(\pm 0.2)\times 10^{-39}$ $mL^2 \cdot molecules^{-2} \cdot s^{-1}$ at $297\pm 1^{\circ}K$. Thus, the second order reaction rate constant respect to Hg^0 and Cl_2, k_g, is $1.82(\pm 0.05)\times 10^{-19}$ $mL \cdot molecules^{-1} \cdot s^{-1}$ at 1 atm and $297\pm 1^{\circ}K$.

The gas phase rate constant obtained in this study is more than three orders of magnitude smaller than those obtained by Hall et. al. (25) and one order of magnitude smaller than that of Ariya et. al. (15). We attribute these disagreements to the effect of the surface and photo-induced reactions. Hall et. al were aware of the effect of surface on the Hg^0 reactions. But, they didn't study the magnitude of the surface contribution, and thus reported a rate constant as the upper limit for the gas phase reaction. Ariya et. al. took a great effort to study the effect of surface of the reactor wall. But, it seems that the contribution of the quartz window surface on the Hg^0

oxidation by Cl_2 was not quantitatively evaluated. The surface area of quartz windows employed by Ariya et. al. was about four times larger than those used in this study. Also, the chlorine concentrations used by Ariya et. al. were 5~10 times less than those used here. The low chlorine concentration would make the surface effect more prominent as compared to the gas phase contribution (table 1), which will be discussed quantitatively later (eq 10).

The surface-induced reaction. As discussed and also from Table 2, we can see that the contribution from the reaction on the quartz window surface accounts for a substantial fraction in the overall Hg^0 decay rate. It's contribution increased with the decrease of the reactor volume. Also, we found that the quartz surface had a larger contribution when it was placed in the inflated part of the reactor than in the neck. The former was about twice as large as the latter when $[Cl_2]$ was 6.5×10^{15} molecules·mL^{-1}. This is indicative that a concentration gradient of Hg^0 was expected to develop across the neck section (along the length of L_f in Figure 1) as the reaction proceeded because the quartz surface reaction rate was larger than the gas phase reaction rate. The mass transfer should take place only by the molecular diffusion in an enclosed and undisturbed system. The Hg^0 concentration in the bulk (the spherical bulge of the reactor) was assumed identical. The adsorption and reaction on the reactor wall were negligible because of the coating of the HW. According to the mass balance and diffusion-control-reaction theory (24), the following equation can be obtained for the reaction rate on the quartz surface.

$$A_q R_{sq} = A\frac{D}{L_f}([Hg^0]-[Hg^0]_s) = A_q k_{sq}'[Hg^0]_s = A_q \frac{1}{\frac{L_f}{D}+\frac{1}{k_{sq}'}}[Hg] \qquad (7)$$

where R_{sq} (molecules·cm^{-2}·s^{-1}) is the reaction rate on quartz. L_f and A are the length of the neck and the surface area of quartz or the cross section of neck ($A=A_q$); D is the diffusion

coefficient of Hg^0, which can be estimated by Satterfield model (26); $\frac{L_f}{D}$ and $\frac{1}{k_{sq}'}$ can be regarded as the diffusion resistance and reaction resistance, respectively (24); and α_q in eq 2a was the local concentration distribution coefficient between the bulk gas and the quartz surface; it can be derived from eq 7 as

$$\alpha_q = \frac{[Hg^0]_s}{[Hg^0]} = \frac{1}{1 + \frac{k_{sq}' L_f}{D}} \qquad (8)$$

It is obvious from the eq 8 that α_q depends on both the diffusion rate and reaction rate constant.

The rate constant of the reaction on quartz surface, k_{sq}', can be determined from eq 7 and the data in Figure 4 as shown in Figure 5. It can be seen that k_{sq}' is linearly proportional to the concentration of chlorine. Therefore, the reaction kinetics on the quartz surface can be expressed as:

$$R_{sq} = k_{sq}[Cl_2][Hg^0]_s \qquad (9)$$

where k_{sq} is the second-order rate constant on the quartz surface, and was calculated to be 2.7×10^{-17} $mL^2 \cdot molecules^{-1} \cdot cm^{-2} \cdot s^{-1}$.

The contribution of gas phase reaction to the overall reaction, $\frac{k_g'}{k_T}$, can be evaluated with eq 10, which was derived from eq 6, 7 and 9 since the contribution of adsorption on the surface was small.

$$\frac{k_g'}{k_T} \approx \frac{k_3[M]}{\frac{A_q}{V}\frac{1}{\frac{1}{k_{sq}} + \frac{[Cl_2]L_f}{D}} + k_3[M]} \qquad (10)$$

From eq 10, one can predict the effect of Cl_2 concentration, $[Cl_2]$, the volume of the reactor, V, and the diffusion coefficient, D on $\frac{k_g'}{k_T}$. Increasing the V and/or $[Cl_2]$ would increase the contribution of gas phase reaction, which would result in a decrease of the surface contribution (eq 4 and Table 1). The D will increase with a decrease of the gas pressure, causing a decrease of the Hg^0 diffusion resistance, $\frac{L_f}{D}$. As a result, the gas phase reaction contribution would decrease (eq 10), and the surface reaction contribution would increase (eq 4, 10 and Table 2).

Photo-induced reaction. The pseudo-1st order overall rate constants, k_T, at various Cl_2 concentrations were determined under continuous and intermittent irradiations. Figure 6 shows that the rate constant was larger when the reaction proceeded under a continuous irradiation (comparing the same size of reactors). The surface reaction was no longer dominant in the presence of the more rapid photo-induced reaction.

Similarly, by running experiments in three reactors, each component in k_T (eq 2a) can be calculated, given the fact that the gas phase rate constant k_g' had been determined at the corresponding conditions. The results are summarized in Table 3. It can be seen that the apparent rate constant of the Hg^0 oxidation on quartz surface, $\alpha_q k_{sq}'$, was almost the same as that of the oxidation without uv-irradiation (shown in Table 1). Consequently, the photo-induced gas reaction rate must be more rapid than the gas reaction rate without the irradiation, given the fact that the overall rate constants are greater under the continuous irradiation. The pseudo-first order rate constant of the photo-induced gas reaction was calculated to be 17.8×10^{-3} s^{-1} at 760 Torr and an intensity of 6.06×10^{16} photons·cm^{-2}·s^{-1}, which was about 16 times larger than that of the gas phase reaction, k_g' (see Table 1) when $[Cl_2]$ was 6.5×10^{15} molecules·mL^{-1}.

Similar to the gas phase reaction, the photo-induced reaction rate appeared to be linearly dependent on the gas pressure, which suggests that the reaction is also a three-body collision process.

$$Hg^0 + h\nu\,(253.7nm) \rightarrow Hg^0* \qquad (11)$$

$$Hg^0* + Cl_2 + M \rightarrow HgCl_2 + M \qquad (12)$$

The use of mercury resonance absorption at 253.7 nm for the measurement of the Hg^0 concentration produces the $Hg^0(6^3P_1)$ excited state (21). The radiative life time of the $Hg^0(6^3P_1)$ state in the transition to the $Hg^0(6^1S_0)$ ground state is 1.03×10^{-7} sec (27, 28). However, the $Hg^0(6^3P_1)$ excited atoms can be quenched rapidly by a third body to produce the $Hg(6^3P_0)$ metastable state (22). The quenching rate constant for this non-radiative transition is 7.1×10^{-12} mL·molecules^{-1}·s^{-1} at 1 atm. N_2, which corresponds to Hg^0 (6^3P_1) half life of about 5×10^{-9} s. Consequently, the non-radiative transition from the $Hg^0(6^3P_1)$ state to the $Hg^0(6^3P_0)$ metastable state would be the dominant process under our experimental conditions. Since the radiative transition of $Hg^0(6^3P_0)$ to $Hg^0(6^1S_0)$ is doubly forbidden, the lifetime of the $Hg^0(6^3P_0)$ atoms are established by the quenching reactions. The quenching rate constant was determined to be 6.1×10^{-15} mL·molecules^{-1}·s^{-1}. Thus, the $Hg^0(6^3P_0)$ atoms possess a half life of about 5×10^{-6} s at 1 atm. N_2. Furthermore, the excited Hg_2 molecules can be produced in this system. The excited $Hg_2(^3l_u)$ molecules is formed in a triple collision of an $Hg^0(6^3P_0)$ atom, a ground-state $Hg^0(6^1S_0)$ atom and a N_2 molecule (29) . The $Hg_2(^3l_u)$ molecule can then either decay spontaneously to the repulsive ground state with a decay constant comparable to that of the atomic 6^3P_1 resonance state, or it can collide with an N_2 molecule and be transferred to the metastable $Hg_2(^30^-_u)$ state which has a radiative life time exceeding 4.5 m sec. The aforementioned excited Hg^0 (6^3P_1 and

6^3P_0) and Hg_2 (^3l_u and $^30^-_u$) could react with the chlorine if the reactants are irradiated with 253.7 nm. The reaction rate constants of each excited Hg^0 and Hg_2 with chlorine are beyond the scope of this study.

The utilization efficiency of 253.7 nm photons for the oxidation of Hg^0, ϕ_{Hg}, can be calculated according to eq 13 (22).

$$\phi_{Hg} = \frac{\text{number of } Hg^0 \text{ molecules oxidized}}{\text{number of photons absorbed by } Hg^0} \qquad (13)$$

The number of the photons absorbed by Hg^0 can be calculated according to the Beer-Lambert law (22).

$$I_a = I_0 \times (1 - 10^{-\sigma L[Hg^0]}) \qquad (14)$$

where I_0 and I_a are, respectively, the inlet photon energy and the energy absorbed by Hg^0 in the reactor, photon·cm^{-2}·s^{-1}. σ is 4.5×10^{-16} cm^2·molecules^{-1} (25), the absorption cross section of Hg^0 at 253.7 nm. L is the optical length of the reactor, cm. [Hg^0] is the concentration in the reactor, molecule·mL^{-1}. Therefore, eq 13 can be written as:

$$\phi_{Hg} = \frac{k_p' V_p [Hg]}{(A_q/2) I_0 (1 - 10^{-\sigma L[Hg]})} \overset{\sigma LC \ll 1}{=} \frac{k_p' V_p}{1.15 \sigma I_0 L A_q} \qquad (15)$$

where $A_q/2$ is the area of one quartz window, through which the light passes into the reactor, V_p was defined in eq 2a or 3. Because the concentration of Hg^0 was very small, $\sigma L[Hg^0]$ was far less than 1 under the experimental conditions. Consequently, the term of $(1 - 10^{-\sigma L[Hg^0]})$ can be approximately expressed as $2.3\sigma L[Hg^0]$ by means of the Taylor law. Therefore, the value of ϕ_{Hg} was calculated to be 6.7×10^{-4} molecules·photon^{-1}, when [Cl_2] was 6.5×10^{15} molecules·mL^{-1} at 1

atm. This result indicated that the utilization efficiency of 253.7 nm photons for the oxidation of Hg^0 is very small.

From this study**,** we found that the oxidation of Hg^0 by Cl_2 can occur by means of three concurrent reaction pathways: gas phase, solid surface, and photo-induced mechanisms. The reaction rate of each mechanism was elucidated by performing experiments using three reactors having different surface area to volume ratios. The photo-induced reaction rate was obtained by comparing results from experiments under continuous and intermittent light illumination. The ternary gas phase oxidation rate constant of Hg^0 by Cl_2 was determined to be $7.5(\pm0.2) \times10^{-39}$ $mL^2 \cdot molecules^{-2} \cdot s^{-1}$ at $297\pm1^\circ K$ and N_2 the balance, which corresponds to a second order rate constant of $1.82(\pm0.05) \times10^{-19}$ $mL \cdot molecules^{-1} \cdot s^{-1}$ at 1 atm N_2. This result is smaller than those determined by Ariya ($2.6(\pm0.2) \times10^{-18}$ $mL \cdot molecules^{-1} \cdot s^{-1}$) and Hall ($<1.6\times 10^{-16}$ $mL \cdot molecules^{-1} \cdot s^{-1}$). The rate constant of the quartz surface-induced oxidation of Hg^0 by Cl_2 was determined to be 2.7×10^{-17} $mL^2 \cdot molecules^{-1} \cdot cm^{-2} \cdot s^{-1}$. The photo-induced oxidation of Hg^0 by Cl_2 accounts for a substantial fraction of Hg^0 oxidation under the experimental conditions employed, however, the utilization efficiency of 253.7 nm photon for Hg^0 oxidation was only 6.7×10^{-4} $molecules \cdot photon^{-1}$ under the conditions employed in this study.

Acknowledgments

This work was supported by the Assistant Secretary for Fossil Energy, U.S. Department of Energy, under Contract DE-AC03-76SF0098 through the National Energy Technology Laboratory.

Literature Cited

1. Davidson R.M.; Clarke L.; Trace elements in coal. IEAPER/21, London, UK, IEA Coal Research, **1996**, Jan., 60 pp.
2. Mercury Study Report to Congress; EPA-452/R-97-008; U.S. Environmental Protection Agency, Office of Research and Development, U.S. Government Printing Office: Washington, DC, December, **1997**; Vol 5.
3. United Nations Environment Programme (UNEP), Global Mercury Assessment, UNEP Chemicals, Geneva, Switzerland (December 2002).
4. Schaefer, J.K.; Yagi, J.; Reinfelder, J.R.; Cardona, T.; Ellickson, K.M.; Tel-or, S. and Barkay, T. *Environ. Sci. Techol*. **2004**, 38, 4304.
5. Clear, R.; Berman, S. *J. Illuminating Eng. Society*, **1994**, 23, 138.
6. Wang, Q; Shen, W.; Ma, Z. *Environ Sci. Techol.* **2000**, 34, 2711.
7. Sloss, L.L. Mercury – Emissions and Control. ISBN 92-9029-371-3, London, UK, IEA Coal Research, Feb. **2002**.
8. Senior, C.L.; Sarofim, A.F.; Zeng, T.; Helble, J.; Mamani-Paco, R. *Fuel Processing Technology*, **2000**, 63,197.
9. Galbreath, K.C.; Zygarlicke, C.J. *Environ Sci. Techol.,* **1996**, 30, 2421.
10. Givelet, N.; Roos-Barraclough, F.; Goodsite M. E.;Cheburkin A. and Shotyk W. *Environ, Sci. Techol*. **2004**, 38, 4964.
11. Schroeder, W.H.; Munthe, J.; *Atmos. Environ.* **1998**, 32, 809.
12. Seigneur, C.; Wrobel, J.; Constantinou, E. *Environ. Sci. Technol.* **1994**, 28, 1589.
13. Tokos, J.J.S.; Hall, B.; Calhoun, J.A.; Prestbo, E.M. *Atmos. Envrion*. **1998**, 32, 823.
14. Lin, C. J.; Pehkonen, S.O. *Atmos. Environ,* **1999**, 33, 2067.

15. Ariya, P.A.; Khalizov, A.; Gidas, A. *J. Phys. Chem.* A **2002**, 106, 7310.

16. Chang, J.C.; Ghorishi, S. B. *Environ. Sci. Technol.* **2003**, 37(24), 5763.

17. Granite, E.J., Pennline, H.W. *Ind. Eng. Chem. Res.* **2002**, 41, 5470.

18. Blythe, G.; Richardson, C.; Rhudy, R. *In Proceedings of Air Quality III*: Mercury, Trace Elements, and Particulate Matter Conference, Arlington, VA, Sept. 9-12, **2002**.

19. Schroeder, W.H.; Yarwood, G.; Niki, H. *Water, Air, Soil Pollut*. **1991**, 56, 653.

20. Iverfeldt, A.; Lindqvist, O. *Atmos. Environ*. **1986**, 20, 1567.

21. Hall, B. Ph.D. Dissertation, Chalmers University of Technology, Goteborg, University of Goteborg, Sweden, **1992**.

22. Calvert, J.G.; Pitts, J.N.; *Photochemisty*, John Wiley & Sons Inc.: New York, **1966**.

23. Hall, B.; Schager, P.; Lindqvist, P. *Water, Air and Soil Pollution*. **1995**, 81, 121.

24. Levenspiel O. Chemical Reaction Engineering**,** John Wiley & Sons Inc: New York, **1998**.

25. Hall, B.; Schager, P.; Lindqvist, P. *Water, Air and Soil Pollution*.**1991**, 56, 3.

26. Satterfield **C.;** Mass Transfer in Heterogeneous Catalysis, MIT press: Cambridge,**1969**.

27. Tolman, R. *Phy. Rev.,* **1924**, 23, 693.

28. Blagoev, K.; Bogdanovich, P.; Dimitrov, N. Momkauskaite, A. *Phy. Rev. A.,* **1988**, 37, 4679.

29. Skonieczny, J.; Krause, L. *Phy. Rev. A.,* **1974**, 9, 1612.

Figure Captions

FIGURE 1. Schematic diagram of the experimental system

FIGURE 2. Semilogarithmic plots of changes of the relative Hg^0 concentrations, due to the adsorption of Hg^0 on the reactor surface, over time at 297±1°K. Three reactor sizes were studied: small reactor with 190 mL volume and 190 cm^2 surface area, medium with 380 mL and 255 cm^2, and large with 960 mL and 498 cm^2. The effect of the surface coating by the halocarbon wax was studied. The initial mercury concentration, $[Hg^0]_0$, employed was 4.4×10^{12} molecules·mL^{-1}.

FIGURE 3. The overall Hg^0 depletion rates in the presence of Cl_2 at various conditions at 297°K. It plots the semilogarithmic changes of the relative Hg^0 concentrations over time. The effect of reactor sizes, surface coating, and uv irradiation on the Hg^0 depletion rates was shown. The initial concentration of Hg^0 and Cl_2 was 4.4×10^{12} molecules·mL^{-1} and 6.5×10^{15} molecules·mL^{-1}, respectively.

FIGURE 4. The overall rate constants as a function of gas pressure from 120 Torr to 770 Torr in three sizes of reactors. The initial Hg^0 and Cl_2 concentrations were 4.4×10^{12} molecules·mL^{-1} and 6.5×10^{15} molecules·mL^{-1}, respectively. All the reactors were coated with halocarbon wax.

FIGURE 5. The rate constant of the reaction of Hg^0 with Cl_2 on the quartz surface as a function of the concentration of chlorine between $1.2x10^{15}$ molecule·mL^{-1} and $13x10^{15}$ molecule·mL^{-1}.

FIGURE 6. The effect of 253.7 nm photon on the overall Hg^0 reaction rate constants with Cl_2 in three sizes of reactors. The Cl_2 concentrations studied were between $1.2x10^{15}$ molecule·mL^{-1} and $13x10^{15}$ molecules·mL^{-1}. ···· indicates the continuous uv-irradiation with the intensity of 6.06×10^{16} photons·cm^{-2}·s^{-1}; — represents the intermittent uv-irradiation. All the reactors were coated with halocarbon wax.

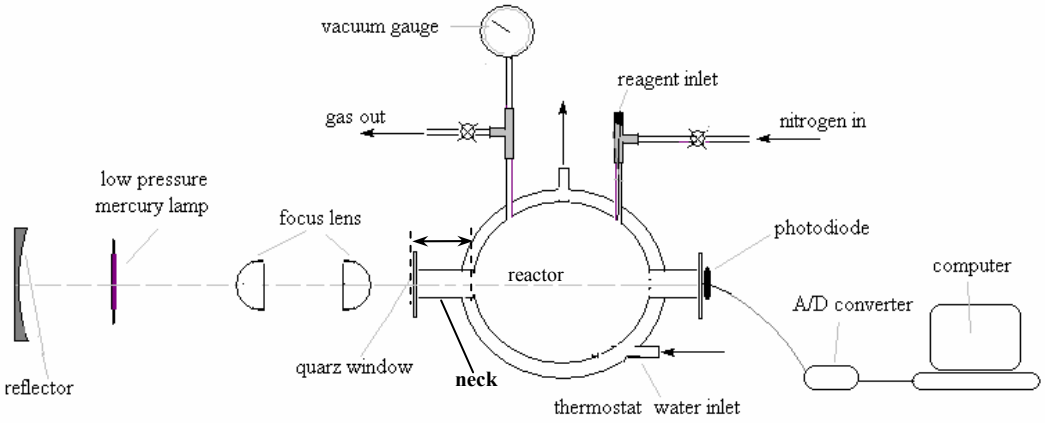
vacuum gauge
reagent inlet
gas out
nitrogen in
low pressure
mercury lamp
focus lens
photodiode
reactor
computer
A/D converter
reflector
quarz window
neck
thermostat
water inlet

FIGURE 1

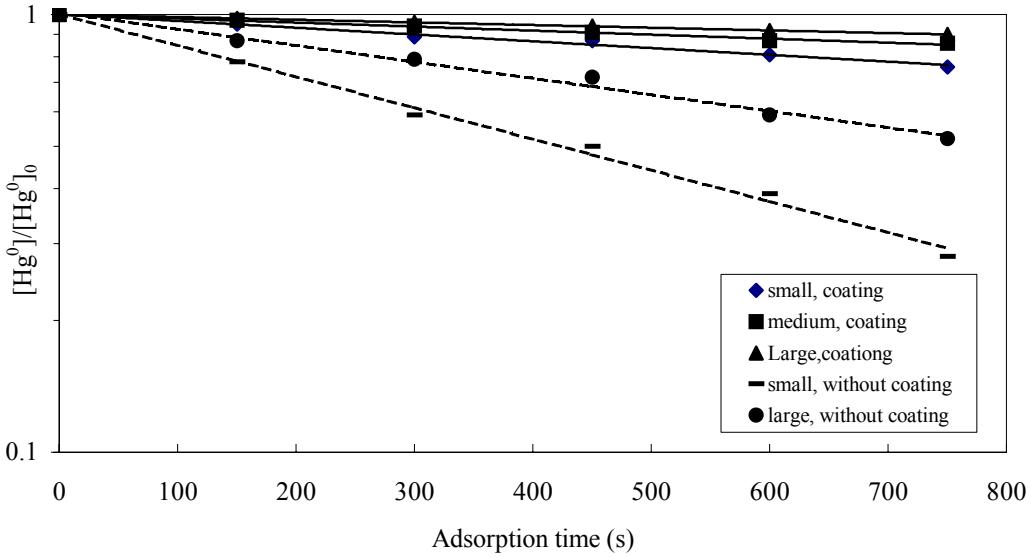
1
0.1
[gH]/[gH]0
0
100
200
300
400
500
600
700
800
Adsorption time (s)
small, coating
medium, coating
Large,coationg
small, without coating
large, without coating

FIGURE 2

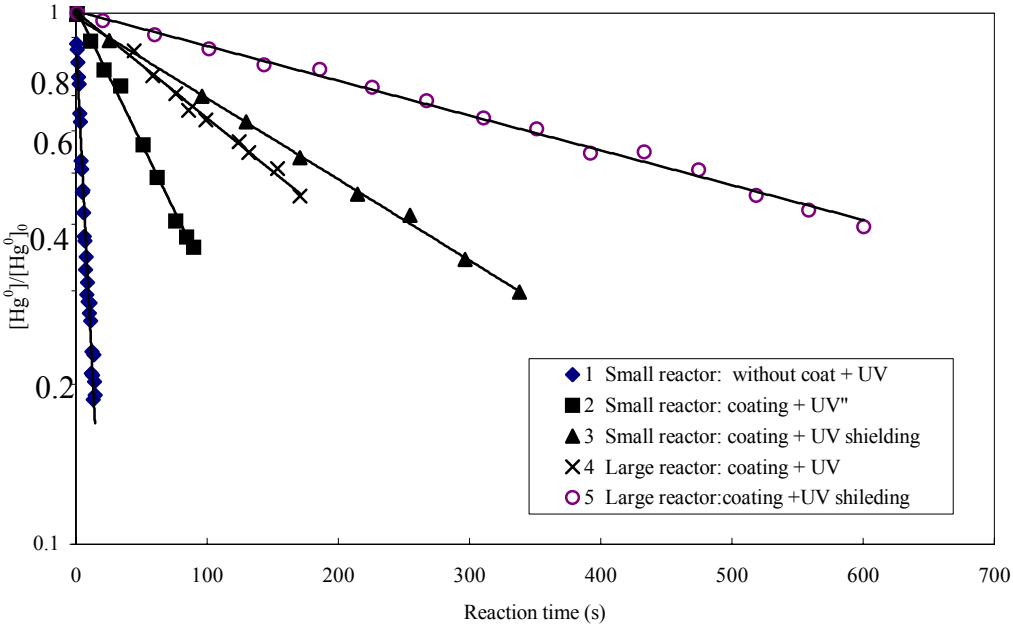
1
0.8
0.6
0.4
0.2
0.1
[Hg0]/[Hg0]0
0
100
200
300
400
500
600
700
Reaction time (s)
1 Small reactor: without coat + UV
2 Small reactor: coating + UV"
3 Small reactor: coating + UV shielding
4 Large reactor: coating + UV
5 Large reactor:coating +UV shileding

FIGURE 3

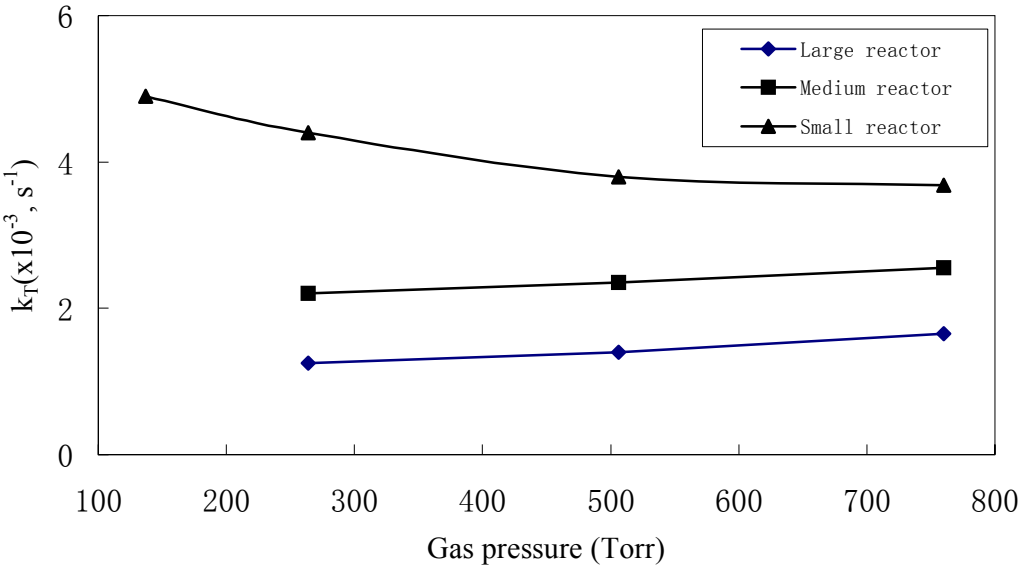
6
4
2
0
100
200
300
400
500
600
700
800
Gas pressure (Torr)
$k_T(x10^{-3}, s^{-1})$
Large reactor
Medium reactor
Small reactor

FIGURE 4

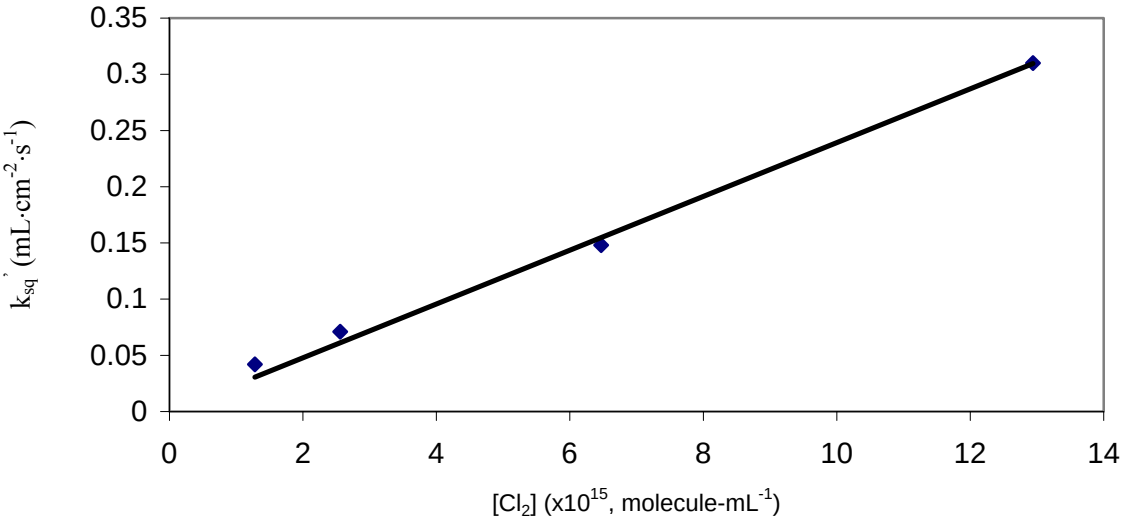
0.35
0.3
0.25
0.2
0.15
0.1
0.05
0
0
2
4
6
8
10
12
14
k_{sq}' (mL·cm^{-2}·s^{-1})
[Cl_2] (x10^{15}, molecule-mL^{-1})

FIGURE 5

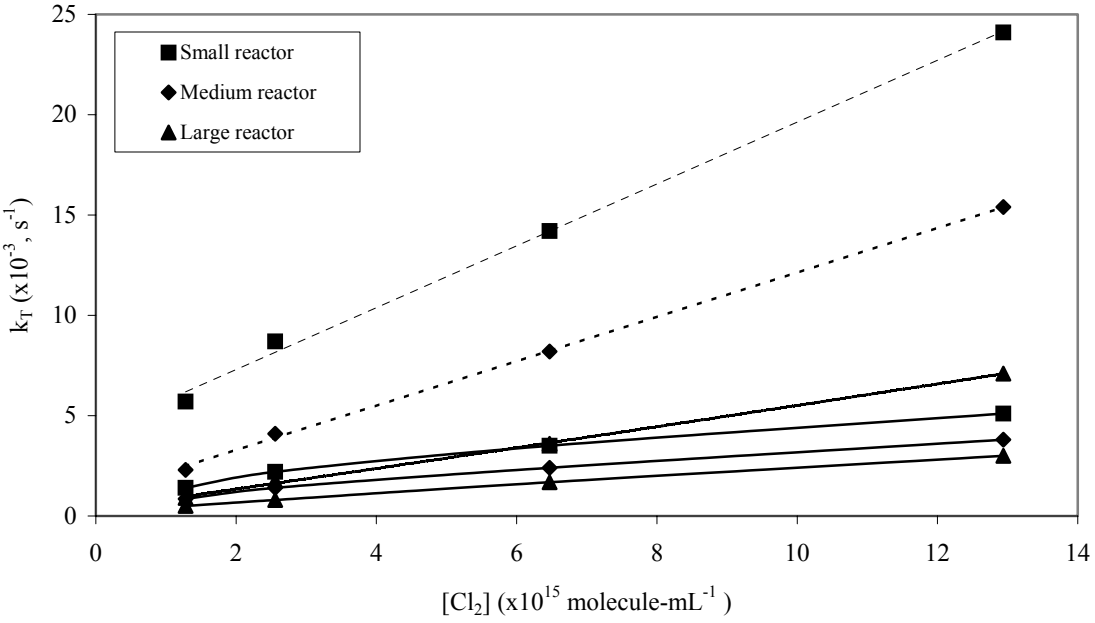
Small reactor
Medium reactor
Large reactor
k_T (x10^{-3}, s^{-1})
$[Cl_2]$ (x10^{15} molecule-mL^{-1})
0
5
10
15
20
25
0
2
4
6
8
10
12
14

Figure 6

TABLE 1. The calculated results of k_g', $\alpha_q k_{sq}'$ and $\alpha_w (k_{aw}+k_{sw}')$ * for gas phase and surface reaction pathways of Hg^0 with Cl_2 from three reactors with various $[Cl_2]$ at 1 atm..

$[Cl_2]$ (molecule s· mL^{-1})	V (mL)	k_g' ($\times10^{-3}$, s^{-1})	$\alpha_q k_{sq}'$** ($\times10^{-3}$, $mL\cdot cm^{-2}\cdot s^{-1}$)	$\alpha_w (k_{aw}+k_{sw}')$ ($\times10^{-3}$, $mL\cdot cm^{-2}\cdot s^{-1}$)	k_g'/k_T *** (%)	$k_g'/[Cl_2]$ ($\times10^{-19}$, $mL\cdot molecules^{-1}\cdot s^{-1}$)
	190				33.1%	
6.5×10^{15}	380	1.2±0.05	49.1±1.0	0.28±0.02	51.3%	1.85± 0.05
	960				71.1%	
	190				21.0%	
2.5×10^{15}	380	0.46±0.03	33.5±1.0	0.28±0.01	34.4%	1.80± 0.05
	960				58.7%	
	190				17.1%	
1.3×10^{15}	380	0.24±0.03	22.5±1.0	0.27±0.01	26.6%	1.82± 0.05
	960				50.5%	

* k_g', k_{sq}', k_{sw}' represent the pseudo-1st rate constants of gas phase reaction, surface reaction on the quartz and the halocarbon wax coated wall, respectively.

** $\alpha_q k_{aq}$ was neglected because it was much smaller than $\alpha_q k_{sq}'$.

*** k_g'/k_T is the ratio of the contribution of gas phase reaction to the overall reaction.

TABLE 2. The effect of gas pressure on k_g' and $\alpha_q k_{sq}'$ for gas phase and surface reaction pathways of Hg^0 with Cl_2 at 297±1°K. $[Cl_2]$ at 6.5×10^{15} molecules·cm^{-3}.

gas pressure (Torr)	V (mL)	k_g' ($\times10^{-3}$, s^{-1})	$\alpha_q k_{sq}'$ ($\times10^{-3}$, mL·cm^{-2}·s^{-1})	k_g'/k_T (%)	$k_g'/[Cl_2]$ ($\times10^{-19}$, mL·molecules^{-1}·s^{-1})
506	190	0.8±0.05	64.2	22.8%	1.20± 0.1
	380			35.3%	
	960			64.3%	
264	190	0.43±0.03	88.5	10.9%	0.66± 0.08
	380			21.1%	
	960			39.2%	

TABLE 3. The effect of gas pressure on photo-induced pseudo-1st rate constant (k_p') and surface reaction on quartz ($\alpha_q k_{sq}'$) at a light intensity of 6.06×10^{16} photons·cm^{-2}·s^{-1} at 297±1°K. [Cl_2] at 6.5×10^{15} molecules·cm^{-3}.

gas pressure (Torr)	k_p' ($\times10^{-3}$, s^{-1})	$\alpha_q k_{sq}'$ ($\times10^{-3}$, mL·cm^{-2}·s^{-1})
760	17.8±0.5	53.4
264	6.4±0.3	91.7